J|A|C|S
ARTICLES
Published on Web 08/19/2006

Binding Free Energy Contributions of Interfacial Waters in HIV-1 Protease/Inhibitor Complexes

Yipin Lu,[†,‡] Chao-Yie Yang,[‡] and Shaomeng Wang*[,†,‡,§]

Contribution from the Departments of Medicinal Chemistry, Internal Medicine, and Pharmacology, University of Michigan, Ann Arbor, Michigan 48109

Received November 26, 2005; E-mail: shaomeng@umich.edu

Abstract: Water molecules are commonly observed in crystal structures of protein−ligand complexes where they mediate protein−ligand binding. It is of considerable theoretical and practical importance to determine quantitatively the individual free energy contributions of these interfacial water molecules to protein−ligand binding and to elucidate factors that influence them. The double-decoupling free energy molecular dynamics simulation method has been used to calculate the binding free energy contribution for each of the four interfacial water molecules observed in the crystal structure of HIV-1 protease complexed with KNI-272, a potent inhibitor. While two of these water molecules contribute significantly to the binding free energy, the other two have close to zero contribution. It was further observed that the protonation states of two catalytic aspartate residues, Asp25 and Asp125, strongly influence the free energy contribution of a conserved water molecule Wat301 and that different inhibitors significantly influence the free energy contribution of Wat301. Our results have important implications on our understanding of the role of interfacial water molecules in protein−ligand binding and to structure-based drug design aimed at incorporating these interfacial water molecules into ligands.

Introduction

Our recent analysis of 392 high-resolution X-ray crystal structures of ligand−protein complexes[1] showed that in some 95% of the complexes there is at least one ligand-bound water molecule and, on average, between three and four water molecules are involved in bridging hydrogen bonds between a protein and its ligand.[1]

When a water molecule is localized in the protein−ligand interface, there is an enthalpy gain from the interaction between the water and the protein−ligand complex. This enthalpy gain is opposed by an entropy cost arising from the restriction in the freedom of movement of both the water and the protein−ligand complex. The upper bound of the entropy cost associated with transfer of a water molecule from bulk solvent to protein has been estimated to be 2.1 kcal/mol.[2] Similarly, based on the data from anhydrous salts and the corresponding hydrates, the enthalpy associated with such water transfer is estimated to be −3.8 kcal/mol,[3] and thus, transfer of a water molecule from bulk solvent to protein could be accompanied by a favorable gain in free energy. Indeed, Li and Lazaridis used statistical mechanics and inhomogeneous fluid solvation theory to estimate the contribution of a bound water molecule to the thermodynamics of protein solvation.[4,5] It was shown that the entropic penalty of ordering, although considerable, is outweighed by the favorable enthalpy gain of the water−complex interactions for two different protein−ligand complex systems.[4,5] Several other groups have used molecular dynamics (MD) free energy simulation to study the water molecules in internal protein cavities.[6−10] In general, it was found that, for a protein cavity containing an experimentally observed water molecule, the free energy change of transferring a water molecule from the bulk solvent to the cavity was calculated to be favorable (i.e., negative), while the free energy change on hydrating an empty cavity was calculated to be unfavorable. Hamelberg and McCammon recently used the double-decoupling method to calculate the standard free energy of sequestration of water molecules in the binding site of protein−ligand complexes.[11] Their study showed that the standard free energy associated with localization of a water molecule in the binding site is −1.9 ± 0.5 kcal/mol for the trypsin/benzylamine complex and −3.1 ± 0.6 kcal/mol for the HIV-1 protease/KNI-272 complex, respectively, suggesting that localization of a water molecule at the binding site stabilizes the protein−ligand complex.

[†] Department of Medicinal Chemistry.
[‡] Department of Internal Medicine.
[§] Department of Pharmacology.

(1) Lu, Y.; Wang, R.; Yang, C. Y.; Wang, S. *J. Chem. Inf. Model*. Manuscript submitted.
(2) Dunitz, J. D. *Science*. **1994**, *264*, 670−671.
(3) Connelly, P. R. *Structure-Based Drug Design: Thermodynamics, Modeling and Strategy*; Ladbury, J. E., Connelly, P. R., Eds.; Springer-Verlag: Berlin, Heidelberg, New York, 1997; Chapter 5, pp 143−159.
(4) Li, Z.; Lazaridis, T. *J. Phys. Chem. B* **2005**, *109*, 662−670.
(5) Li, Z.; Lazaridis, T. *J. Am. Chem. Soc.* **2003**, *125*, 6636−6637.
(6) Olano, R.; Rick, W. *J. Am. Chem. Soc.* **2004**, *126*, 7991−8000.
(7) Wade, R.; Mazor, M.; McCammon, J.; Quiocho, F. *Bioplymers* **1991**, *31*, 919−931.
(8) Roux, B.; Nina, M.; Pomès, R.; Smith, J. *Biophys. J.* **1996**, *71*, 670−681.
(9) Zhang, L.; Hermans, J. *Proteins: Struct., Funct., Genet.* **1996**, *24*, 433−438.
(10) Helms, V.; Wade, R. *Biophys. J.* **1995**, *69*, 810−824.
(11) Hamelberg, D.; McCammon, J. A. *J. Am. Chem. Soc.* **2004**, *126*, 7683−7689.

10.1021/ja058042g CCC: $33.50

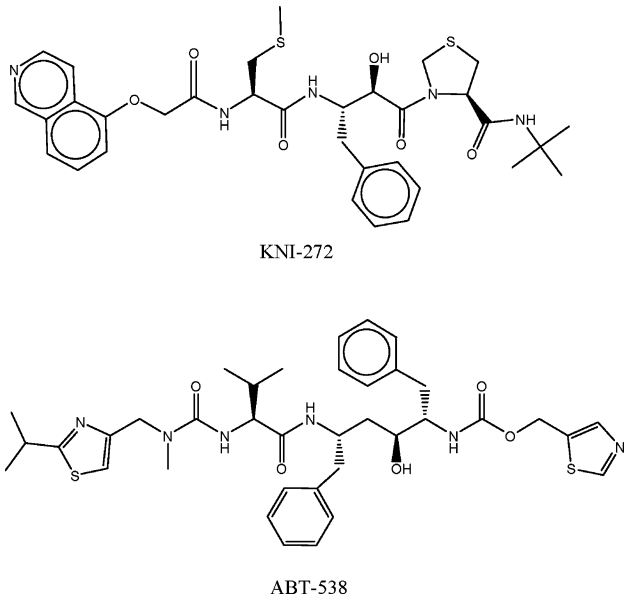

Figure 1. Chemical structures of two HIV-1 protease inhibitors KNI-272 and ABT-538.

Although theoretical studies have provided important insights into the contributions of interfacial water molecules to protein−ligand interactions, our knowledge is still limited, and many important questions remain unanswered. For example, since a protein−ligand complex contains on average three to four interfacial bridging water molecules,[1] it is of both theoretical and practical importance to determine the binding free energy contribution for each individual water molecule because this contribution could be a significant part of the overall binding free energy. Furthermore, factors that influence the free energy contribution for individual water molecules remain to be elucidated.

To address these questions, we have performed a computational study to investigate the free energy contribution of several interfacial water molecules in HIV-1 protease (HIV-1 PR) in a complex with Kynostatin 272 (KNI-272). KNI-272 (Figure 1) is a potent and selective inhibitor of HIV-1 PR, with a K_i value of 5.5 pM.[12] Four water molecules, Wat301, Wat566, Wat607, and Wat608, have been observed crystallographically at the interface between HIV-1 PR and KNI-272[13] (Figure 2). NMR spectroscopy has indeed confirmed the presence of these four water molecules in the solution structure of the complex, indicating that these water molecules, which are also observed in the crystal structure of HIV-1 PR complexed with KNI-272, are not an artifact of the crystallization process.[14] The HIV-1 PR/KNI-272 complex system therefore provides an excellent example with which to study the free energy contribution of individual interfacial water molecules to protein−ligand binding.

Among the four interfacial water molecules in the HIV-1 PR/KNI-272 complex,[13] Wat301 has been found to bridge the gaps between flaps of HIV-1 PR and KNI-272. This water molecule, functioning as an acceptor, forms two hydrogen bonds with the

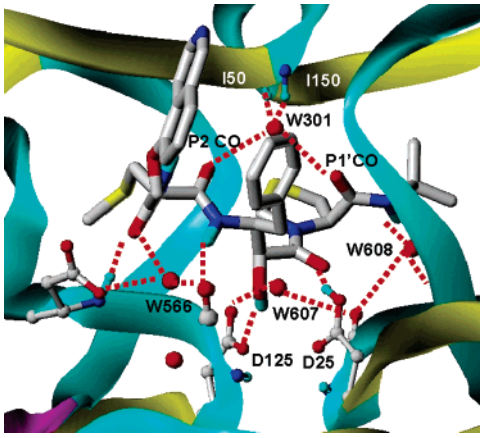

Figure 2. Four interfacial water molecules observed at the crystallographic structure of HIV-1 protease complexed with KNI-272 (1hpx). The inhibitor KNI-272 is in capped stick and the HIV-1 protease residues are in ribbon and ball-and-stick. The hydrogen bonds formed between the interface water molecules and the complex are shown as red dashed lines.

NH groups of Ile50 and Ile150 in HIV-1 PR and at the same time, functioning as a donor, forms two additional hydrogen bonds with the CO groups at the P1′ and P2 sites of the bound inhibitor.[13] This bridging water Wat301 thus plays a critical role in the interaction between HIV-1 PR and its inhibitor and is in fact observed in nearly all HIV PR/inhibitor complexes,[15] except in cases in which it is displaced deliberately in the design of the inhibitors.[16] To investigate if an inhibitor bound to HIV-1 PR influences the free energy contribution of Wat301, we have also employed HIV-1 PR in complex with ABT-538[17] as our second model system (Figure 3). ABT-538 (ritonavir, Figure 1) is another potent and selective HIV-1 PR inhibitor with a K_i value of 15 pM and is marketed as a drug for the treatment of HIV-1 infection. Of note, ABT-538 and KNI-272 belong to two different chemical classes (Figure 1).

In the HIV-1 PR/KNI-272 complex, two catalytic aspartate residues Asp25 and Asp125 directly interact with the inhibitor but not with Wat301. An NMR study of the HIV-1 PR/KNI-272 complex indicated that the Asp25 is protonated while Asp125 is deprotonated.[18] However, another NMR study showed that Asp25 and Asp125 are both protonated when HIV-1 PR is bound to a non-peptide cyclic urea-based inhibitor, which incorporated Wat301 into the inhibitor.[19] The protonation states of these two catalytic residues were shown to influence the calculated relative binding free energy of HIV-1 PR inhibitors.[20,21] Accordingly, we have investigated the influence of the protonation states of Asp25 and Asp125 on the binding free energy contribution of Wat301 in the HIV-1 PR/KNI-272 complex.

We employed the double-decoupling free energy simulation method[11,22] to calculate the free energy contribution of individual interfacial water molecules. This method[11,22] is based on an

(12) Kageyama, S.; Mimoto, T.; Murakawa, Y.; Nomizu, M.; Ford Jr, H.; Shirasaka, T.; Gulnik, S.; Erickson, J.; Takada, K.; Hayashi, H. *Antimicrob. Agents. Chemother*. **1993**, *37*, 810−817.
(13) Baldwin, E. T.; Bhat, T. N.; Gulnik, S.; Liu, B.; Topol, I. A.; Kiso, Y.; Mimoto, T.; Mitsuya, H.; Erickson, J. W. *Structure* **1995**, *3*, 581−590.
(14) Wang, Y. X.; Freedberg, D. I.; Wingfield, P. T.; Stahl, S. J.; Kaufman, J. D.; Kiso, Y.; Bhat, T. N.; Erickson, J. W.; Torchia, D. A. *J. Am. Chem. Soc.* **1996**, *118*, 12287−12290.
(15) Wlodawer, A.; Erickson, J. *Annu. Rev. Biochem.* **1993**, *62*, 543−585.
(16) Lam, P. Y. S.; et al. *Science* **1994**, *263*, 380−384.
(17) Kempf, D. J.; et al. *Proc. Natl. Acad. Sci. U.S.A.* **1995**, *92*, 2484−2488.
(18) Wang, Y. X.; Freedberg, D. I.; Yamazaki, T.; Wingfield, P. T.; Stahl, S. J.; Kaufman, J. D.; Kiso, Y.; Torchia, D. A. *Biochemistry* **1996**, *35*, 9945−9950.
(19) Yamazaki, T.; et al. *J. Am. Chem. Soc.* **1994**, *116*, 10791−10792.
(20) Chen, X.; Tropsha, A. *J. Med. Chem.* **1995**, *38*, 42−48.
(21) Ferguson, D. M.; Radmer, R. J.; Kollman, P. A. *J. Med. Chem.* **1991**, *34*, 2654−2659.
(22) Gilson, M. K.; Given, J. A.; Bush, B. L.; McCammon, J. A. *Biophys. J.* **1997**, *72*, 1047−1069.

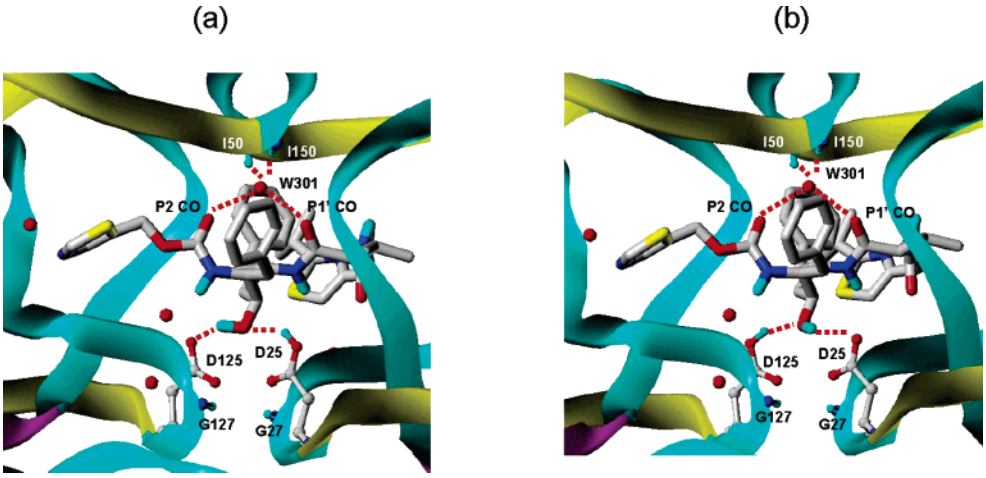

Figure 3. Wat301 observed at the crystallographic structure of HIV-1 protease complexed with ABT-538 (1hxw) as (a) Asp25 protonated and Asp125 deprotonated, (b) Asp125 protonated and Asp25 deprotonated. The inhibitor ABT-538 is in capped stick and the HIV-1 protease residues are in ribbon and ball-and-stick. The hydrogen bonds formed between the interface water molecuels and the complex are shown as red dashed lines.

underlying principle of statistical thermodynamics and has been shown to be theoretically sound for free energy calculations. Hamelberg and McCammon[11] have successfully employed this method to calculate the free energy contributions of water molecules in two protein−ligand complexes.

Our study showed that two of the four interfacial water molecules in the HIV-1 PR/KNI-272 complex make significant contributions to the overall protein−ligand binding free energy, while the other two water molecules make minor contributions. Our calculations also indicate that the free energy contribution of Wat301 to protein−ligand binding is strongly influenced by the bound inhibitor and the protonation states of the two catalytic aspartate residues Asp25 and Asp125. Our study thus suggests that some but not all interfacial water molecules make significant contributions to the protein−ligand binding free energy, and the local environment strongly influences the free energy contribution associated with any specific interfacial water molecule.

Methods

Double-Decoupling Free Energy Simulation. The double-decoupling approach[11,22] was employed to calculate the free energy contribution ($\Delta G°$) of interfacial water molecules in the binding site of the HIV-1 PR complexed with either KNI-272 or ABT-538. The value of $\Delta G°$ is determined as the difference between ΔG_2° and ΔG_1° ($\Delta G_2^\circ - \Delta G_1^\circ$), where ΔG_1° is the free energy change associated with removal of a water molecule (W) to the gas phase from the protein (P) complexed with the ligand (L) in solution (eq 1) and ΔG_2° is the free energy change of removal of a water molecule from the bulk solvent to the gas phase (eq 2)

$$\mathrm{P \cdot W \cdot L\ (sol)} \xrightarrow{\Delta G_1^\circ} \mathrm{P \cdot L\ (sol) + W\ (gas)} \quad (1)$$

$$\mathrm{W\ (sol)} \xrightarrow{\Delta G_2^\circ} \mathrm{W\ (gas)} \quad (2)$$

$$\mathrm{P \cdot L\ (sol) + W\ (sol)} \xrightarrow{\Delta G° = \Delta G_2^\circ - \Delta G_1^\circ} \mathrm{P \cdot W \cdot L(sol)} \quad (3)$$

ΔG_2° is independent of the standard concentration.[11,22] The calculation of ΔG_2° is straightforward and can be computed by thermodynamic integration or by a free energy perturbation approach.[11] In the calculation of the standard free energy associated with removal of a water molecule from the protein to the gas phase (ΔG_1°), the water molecule should explore the entire simulation box for ΔG_1° to converge. This will require prohibitively long simulation times but can be circumvented by applying a harmonic potential to the water molecule to constrain it to the protein site of interest.[11] Correction terms due to the constraining of the water molecule during the free energy simulation are added to the calculated free energy change by thermodynamic integration or free energy perturbation approaches as follows:[11,22]

$$\Delta G_1^\circ = \int \left\langle \frac{\partial U}{\partial \lambda} \right\rangle_\lambda \mathrm{d}\lambda - RT \ln\left(\frac{\sigma_{\mathrm{PLW}}}{\sigma_{\mathrm{PL}}\sigma_{\mathrm{W}}}\right) + RT \ln[C^\circ(2\pi RT/k_{\mathrm{harm}})^{3/2}] + RT \ln(\zeta_{\mathrm{I}}/8\pi^2) + P^\circ(\overline{V_{\mathrm{PL}}} - \overline{V_{\mathrm{PLW}}})$$

$$= \int \left\langle \frac{\partial U}{\partial \lambda} \right\rangle_\lambda \mathrm{d}\lambda + \Delta G_{\mathrm{corr}} \quad (4)$$

where

$$\Delta G_{\mathrm{corr}} = -RT \ln\left(\frac{\sigma_{\mathrm{PLW}}}{\sigma_{\mathrm{PL}}\sigma_{\mathrm{W}}}\right) + RT \ln[C^\circ(2\pi RT/k_{\mathrm{harm}})^{3/2}] + RT \ln(\zeta_{\mathrm{I}}/8\pi^2) + P^\circ(\overline{V_{\mathrm{PL}}} - \overline{V_{\mathrm{PLW}}})$$

$C°$ is the standard concentration, R is the gas constant, and T is absolute temperature. σ_{PLW} is the symmetry number of the protein−ligand complex with the localized water molecule. Similarly, σ_{PL} is the symmetry number of the protein−ligand complex without the localized water molecule, and σ_{W} is the symmetry number of the water molecule. ζ_{I} is the integral over the rotational space sampled by the ideal gas. $\overline{V_{\mathrm{PLW}}}$ is the change in the equilibrium volume when one molecule of the protein−ligand complex (PL) together with the localized water molecule (PLW) is added to n molecules of solvent at standard pressure $P°$. Similarly, $\overline{V_{\mathrm{PL}}}$ is the change in the equilibrium volume when one molecule of protein−ligand complex (PL) without the localized water molecule is added to n molecules of solvent at standard pressure $P°$. The first term in eq 4 is the change in free energy calculated by thermodynamic integration with harmonic force constant k_{harm} on the decoupled water molecule when it is removed from the protein site to the gas phase. The second term accounts for the fact that the water molecule is symmetrical with a symmetry number (σ_{W}) of 2. The third term $RT \ln[C^\circ(2\pi RT/k_{\mathrm{harm}})^{3/2}]$ represents the change in free energy when the gas-phase water molecule, with restrained harmonic potential, is allowed to expand and occupy a volume of $1/C°$. The fourth term $RT \ln(\zeta_{\mathrm{I}}/8\pi^2)$ represents the change in free energy when the rotationally constrained water molecule is allowed to rotate freely. In our simula-

tions, the bound water molecule was allowed to rotate freely, which reduces this term to zero. The last term $P^\circ(\overline{V_{PL}} - \overline{V_{PLW}})$ represents the pressure−volume work associated with the change in volume of the complex−solvent system when the water molecule is decoupled from it in a constant pressure simulation. This contribution is expected to be negligible at normal pressure.[22] Therefore, ΔG_{corr}, the correction term in eq 4, can be rewritten as:

$$\Delta G_{corr} = -RT \ln\left(\frac{\sigma_{PLW}}{\sigma_{PL}\sigma_W}\right) + RT \ln[C^\circ(2\pi RT/k_{harm})^{3/2}] + RT \ln(\zeta_I/8\pi^2) + P^\circ(\overline{V_{PL}} - \overline{V_{PLW}})$$

$$\approx -RT \ln\left(\frac{\sigma_{PLW}}{\sigma_{PL}\sigma_W}\right) + RT \ln[C^\circ(2\pi RT/k_{harm})^{3/2}] \quad (5)$$

The detailed derivation of eq 4 and a thorough description of the double decoupling methodology have been described by Gilson et al.[22] and Hamelberg et al.[11]

The optimal choice for k_{harm} on the decoupled water molecule is such that the force constant should match the mean square positional fluctuation of the unrestrained water molecule in the site of interest during an MD simulation of the fully interacting system without restraints.[11,23] This is defined by eq 5:

$$k_{harm} = \frac{3RT}{\langle \delta r^2 \rangle} \quad (6)$$

where $\langle \delta r^2 \rangle$ is the square of the calculated atomic positional fluctuation in the MD simulation of the fully interacting system without restraints.

Molecular Dynamics Simulation. All MD simulations were performed using the Amber software package (versions 7 and 8).[24,25] The coordinates for the HIV-1 PR/KNI-272 complex[13] (1hpx) and the HIV-1 PR/ABT-538 complex[17] (1hxw) were retrieved from the Protein Data Bank (PDB).[26] An NMR study[18] showed that in the HIV-1 PR/KNI-272 complex, the catalytic acid Asp25 is protonated while Asp125 is deprotonated. A semiempirical quantum mechanical calculation on the ionic states of the catalytic Asp residues[13] further indicated that the protonation of Asp25 is at the OD2 oxygen. Accordingly, we have treated Asp25 in the HIV-1 PR/KNI-272 complex as protonated at OD2 and Asp125 as deprotonated unless otherwise noted. By contrast there is no specific experimental study on the protonation state of the catalytic aspartic acids in the HIV-1 PR/ABT-538 complex. According to the commonly accepted mechanism of the protease reaction,[27,28] only one of the catalytic aspartic acid residues in the HIV-1 protease active site should be protonated, while the other one exists as the anion. Examination of the hydrogen bonding networks in the HIV-1 PR/ABT-538 complex, which includes the catalytic aspartic acids, suggests that the single site of protonation is either the OD2 of the Asp25 or OD2 of the Asp125. Hence, when we studied the role of Wat301 in the HIV-1 PR/ABT-538 complex, we calculated the free energy contribution of Wat301 in two alternative monoprotonation states: protonated at the OD2 of Asp25 or protonated at the OD2 of Asp125.

Atomic charges for KNI-272 and ABT-538 were calculated using RESP methodology[29,30] at the HF/6-31G* level of theory in Gaussian 98.[31] Other force field parameters, including the Lennard-Jones, torsion, and bond angle terms, were taken from the Amber 1999 force field.[32,33]

Each complex was solvated with TIP3P water molecules.[34] Chloride counterions were added into the systems to maintain charge neutrality of the systems. Simulations were performed in the NPT ensemble and with the Berendsen temperature algorithm[35] at a constant temperature of 300 K and a pressure of 1 bar. Solvent molecules and counterions were minimized for 1000 steps with 500 kcal·mol^{-1}·Å^{-2} harmonic constraints placed on inhibitor, protein, and crystallographic water molecules. The whole system was heated from 0 to 300 K over 30 ps with harmonic constraints on the protein, ligand, and crystallographic water molecules. This is followed by equilibration for 100 ps at 300 K with harmonic constraints gradually reduced to zero and an additional 200 ps equilibration of the system without constraints. The equilibrated systems were used to perform 1 ns of MD simulations with periodic boundary conditions. The particle mesh Ewald method[36] was used to treat the long-range electrostatic interactions. A 12 Å cutoff of nonbonded van der Waals interactions and a 2-fs time step were used. Snapshots of the MD trajectories were collected every 1 ps for analysis.

Free energies were calculated using the thermodynamic integration (TI) method at discrete points of λ from 0 to 1, with fixed $\Delta\lambda = 0.05$. A 1-fs time step is used. $\lambda = 0$ is the state in which the water molecule has full interaction with the system, whereas $\lambda = 1$ is the state in which the water molecule is "decoupled" and in the gas phase. The free energy change for each simulation was calculated by varying λ forward from 0 to 1 and then backward from 1 to 0. During simulation, the protein may translate and rotate away from the constrained water molecule. Therefore, a small constraint of 2 kcal·mol^{-1}·Å^{-2} was added on the backbone atoms of protein residues 15 Å away from the perturbed water molecule, to maintain the relative positions between protein and perturbed water molecule. An electrostatic decoupling method was used first to turn off the electrostatic interactions and then to turn off the van der Waals interactions. The end configuration of the electrostatic calculation is used as the starting configuration of the van der Waals calculation without additional equilibration. In the backward simulation, the reverse of the above procedure is performed. The forward and the backward simulations are separated by 60 ps of reequilibration except for the calculation of Wat608 (the reason is discussed below).

Since the van der Waals part is more difficult to converge, a nonlinear mixing TI algorithm[24,37] was used to treat it:

$$V(\lambda) = (1-\lambda)^n V_0 + [1-(1-\lambda)^n] V_1$$

If $n = 1$ (linear coupling), the free energy derivative for the van der Waals interaction part diverges at $\lambda = 1$, and special numerical integration techniques are required to obtain a good estimate of the integral; if $n \geq 4$, the derivative remains finite as $\lambda \rightarrow 1$.[24,37] In our study, we chose $n = 4$ for Wat301, Wat607, and Wat566, but used $n = 6$ for Wat608 since, in our simulation, this water has a very weak harmonic potential, a point which is further discussed below. The simulation for each value of λ was equilibrated for 10 ps, and then

(23) Roux, B.; Nina, M.; Pomès R.; Smith J. C. *Biophys. J.* **1996**, *71*, 670−681.
(24) Case, D. A.; et al. *AMBER 8*; University of California: San Francisco, 2004.
(25) Case, D. A.; et al. *AMBER 7*; University of California: San Francisco, 2002.
(26) Berman, H. M.; Westbrook, J.; Feng, Z.; Gilliland, G.; Bhat, T. N.; Weissig, H.; Shindyalov, I. N.; Bourne P. E. *Nucleic Acids Res.* **2000**, 28, 235−242.
(27) Hyland, L. J.; et al. *Biochemistry* **1991**, *30*, 8441−8453.
(28) Suguna, K.; Padlan, E. A.; Simth, C. W.; Carlson, W. D. *Proc. Natl. Acad. Sci. U.S.A.* **1987**, *84*, 7009−7013.
(29) Bayly, C. I.; Cieplak, P.; Cornell, W. D.; Kollman, P. A. *J. Phys. Chem.* **1993**, *97*, 10269−10280.
(30) Cornell, W. D.; Cieplak, P.; Balyl, C. I.; Kollman, P. A. *J. Am. Chem. Soc.* **1993**, *115*, 9620−9631.
(31) Frisch, M. J.; et al. *Gaussian 98*, revision A.9; Gaussian, Inc.: Pittsburgh, PA, 1998.
(32) Cornell, W. D.; Cieplak, P.; Bayly, C. I.; Gould, I. R.; Merz, K. M.; Ferguson, D. M., Jr.; Spellmeyer, D. C.; Fox, T.; Caldwell, J. W.; Kollman, P. A. *J. Am. Chem. Soc.* **1995**, *117*, 5179−5197.
(33) Wang, J.; Cieplak, P.; Kollman, P. A. *J. Comput. Chem.* **2000**, *21*, 1049−1074.
(34) Jorgensen, W. L.; Chandrasekhar, J.; Madura, J. D.; Impey, R. W.; Klein, M. L. *J. Chem. Phys.* **1983**, *79*, 926−935.
(35) Berendsen, H. J. C.; Postma, J. P. M.; van Gunsteren, W. F.; DiNola, A. *J. Chem. Phys* **1984**, *81*, 3684−3690.
(36) Essmann, U.; Perera, L.; Berkowitz, M. L.; Darden, T.; Lee, H.; Pedersen, L. G. *J. Chem. Phys.* **1995**, *103*, 8577−8593.
(37) Simonson, T. Free energy calculations. In *Computational Biochemistry and Biophysics*; Becker, O., MacKerell, A. D., Roux, B., Watanabe, M., Eds.; New York: Marcel Dekker: 2001; pp 169−197.

Table 1. Calculated Standard Free Energy Change for Removal of a Water Molecule from Bulk Water to the Gas Phase

	ΔG_2° (kcal/mol)		
	forward	backward	average
ele[a]	8.4	8.3	
vdw[a]	−2.4	−2.5	
total	6.0	5.8	5.9 ± 0.1

[a] ele: the electrostatic component of the free energy change calculated by the electrostatic decoupling approach. vdw: the van der Waals interaction component of the free energy change calculated by the electrostatic decoupling approach.

sampled for a minimum of 20 ps for Wat301 and Wat607, and a minimum of 40 ps for Wat566 and Wat608.

Results and Discussion

Our calculated standard free energy change for removal of a water molecule from bulk water to the gas phase is 5.9 ± 0.1 kcal/mol (Table 1). This value is close to the experimentally observed free energy change of 6.3 kcal/mol[38] and previously calculated values of 6.0[11] and 6.1 kcal/mol.[39]

The calculated standard binding free energies of different water molecules at the HIV-1 PR/KNI272 interface and HIV-1 PR/ABT538 interface are summarized in Tables 2 and 3. Each term required to calculate the binding free energy according to eqs 4 and 5 is also listed. The sum of the electrostatic (ele) and van der Waals (vdw) terms in Tables 2 and 3 is the free energy change calculated by thermodynamic integration. Two nonzero correction terms are added to this calculated free energy change. The first correction term, $-RT\ \ln(\sigma_{PLW}/\sigma_{PL}\sigma_W)$, accounts for the fact that the water molecule is symmetrical with a symmetry number (σ_W) of 2 and the value of this term is same for every bound water molecule. The second correction term, $RT\ \ln[C^\circ(2\pi RT/k_{harm})^{3/2}]$, accounts for the fact that the translational degrees of freedom of the bound water molecule were constrained with a force constant k_{harm} during the simulation. The value of this term varies according to the strength of k_{harm} on the bound water molecule. It was shown that the strength of the restraining potentials can influence the calculated free energies.[11] An excessively large restraining potential may lead to significantly greater calculated free energy due to the restricted sampling space. On the other hand, a too small restraining potential could cause the simulation to fail to converge properly.[11] In our study, the force constant k_{harm} was accurately estimated by eq 6 based upon the atom positional fluctuation of water molecules in the MD simulation (see Methods section). Our MD simulation indicated that Wat301 has much less positional fluctuation than the other three water molecules, and thus, the calculated force constant k_{harm} for Wat301 is greater than that for Wat607, Wat566, and Wat608.

Free Energy Contribution of Wat301. In both HIV-1 PR/KNI-272[13] and HIV-1 PR/ABT-538[17] crystal structures, Wat301 bridges the flaps of the protein to the inhibitor by accepting two hydrogen bonds from the NH group of Ile50/Ile150 and donating two hydrogen bonds to the carbonyl oxygens at the inhibitor P1′/P2 sites.[15]

Our free energy simulation of the HIV-1 PR/KNI-272 system showed that the standard free energy associated with removal of this water molecule from the protein to the gas phase (ΔG_1°) is 7.8 ± 0.3 kcal/mol (Table 2). The values for ΔG_1° in the forward and backward calculations are 8.0 and 7.5 kcal/mol, respectively, indicative of good convergence in our simulations. Thus, the free energy contribution (ΔG°) associated with binding of this water molecule in the HIV-1 PR/KNI-272 complex is −1.9 ± 0.4 kcal/mol, indicative of a favorable contribution to the overall protein−ligand binding.

Using the same computational method, Hamelberg and McCammon have previously studied the free energy contribution of Wat301 in HIV-1 PR/KNI-272 complex.[11] Their calculated free energy change was −3.1 ± 0.6 kcal/mol, which is 1.2 kcal/mol more favorable than that obtained from our calculation. A critical difference between these two calculations is that both catalytic aspartic acids were treated as deprotonated in the previous study,[11] whereas in our work, Asp25 is treated as protonated and Asp125 as deprotonated based upon the NMR evidence.[18] Hence, the discrepancy between these two results may be due to different assumptions concerning the protonation states of the Asp25 residue.

To investigate this discrepancy further, we performed another free energy calculation for Wat301 with both of the catalytic aspartic acids deprotonated (Table 3). Under this deprotonation condition, our calculated ΔG_1° value is 9.1 ± 0.2 kcal/mol and the free energy contribution (ΔG° in Table 3) for Wat301 is −3.2 ± 0.4 kcal/mol. This is in an excellent agreement with −3.1 ± 0.6 kcal/mol, the value obtained by Hamelberg and McCammon.[11] Our data thus demonstrate that, notwithstanding the considerable distance between Wat301 and Asp25 or Asp125, the protonation states of these two aspartate residues have a strong influence on the calculated binding free energy of Wat301. It should be noted that these two aspartate residues closely interact with the inhibitor, which forms two hydrogen bonds with Wat301.

Since the protonation states of Asp25 and Asp125 have such a strong influence on the binding free energy for Wat301, we have thus performed two 1-ns MD simulations of the HIV-1 PR/KNI-272 complex with the two different protontation states of the Asp25/125: the dianionic model (−1, −1) in which both of the Asp25/Asp125 are deprotonated, and the monoanionic model (0, −1) in which Asp25 is protonated and Asp125 is deprotonated.

In both simulations, the protein system is stable over the 1-ns simulation based upon both structure and potential energy of the system. The root-mean-square deviation (RMSD) of the protein backbone atoms during the MD simulations relative to the crystal structure is depicted in Figure 4. In both cases, the global structure of the protease remains close to crystal structure over the 1-ns simulation (Figure 4 and Supporting Information). However, the protein backbone in the simulation with a deprotonated state for both Asp25 and Asp125 residues deviates more significantly from the crystal structure than in the simulation with monoprotonated state for these two residues (Figure 4 and Figure S1 in the Supporting Information). The dianionic states of Asp 25/125 lead to some significant local structural changes of the protein−ligand complex, as compared to the crystal structure, especially in the active site of the protein and the P1, P1′, and P2′ moieties of the ligand (Figure 5). Due to the strong electrostatic repulsion, the two catalytic aspartic acids are further apart in the doubly deprotonated (−1, −1)

(38) Bennaim, A.; Marcus, Y. J. *Chem. Phys.* **1984**, *81*, 2016−2027.
(39) Jorgensen, W. L.; Blake, J. F.; Buckner, J. K. *Chem. Phys.* **1989**, *129*, 193−200.

Table 2. Standard Binding Free Energies and Their Components of Different Water Molecules in the Interface between HIV-1 PR and KNI-272

			ΔG_1° (kcal/mol)[b]					
					correction			
	k_{harm} (kcal/mol/Å^2)		ele	vdw	$-RT\ln\left(\frac{\sigma_{PLW}}{\sigma_{PL}\sigma_W}\right)$	$RT\ln\left[C^\circ\left(\frac{2\pi RT}{k_{harm}}\right)^{3/2}\right]$	total	$\Delta G^\circ = \Delta G_2^\circ - \Delta G_1^\circ$ (kcal/mol)[c]
Wat301	10	F[a]	11.1	1.8	0.4	−5.3	8.0	
		B	10.4	2.0	0.4	−5.3	7.5	−1.9 ± 0.4
		avg					7.8 ± 0.3	
Wat607	4.5	F	9.9	1.4	0.4	−4.6	7.1	
		B	9.1	1.9	0.4	−4.6	6.8	−1.1 ± 0.3
		avg					7.0 ± 0.2	
Wat566	2.7	F	11.0	−1.6	0.4	−4.0	5.8	
		B	10.8	−2.1	0.4	−4.0	5.1	0.4 ± 0.5
		avg					5.5 ± 0.4	
Wat608	1.0	F	12.5	−3.4	0.4	−3.2	6.3	
		B	13.0	−4.2	0.4	−3.2	6.0	−0.3 ± 0.3
		avg					6.2 ± 0.2	

[a] F: forward; B: backward; avg: average. [b] ele: the electrostatic component of the free energy change calculated by the electrostatic decoupling approach. vdw: the van der Waals interaction component of the free energy change calculated by the electrostatic decoupling approach. Correction: the calculated nonzero correction terms corresponding to the ΔG_{corr} in eqs 4 and 5. [c] $\Delta G_2^\circ = 5.9 \pm 0.1$ kcal/mol, as in Table 1.

Table 3. Standard Binding Free Energies and their Components of Wat301 in Different HIV-1 PR−Inhibitor Complexes with Different Protonation States of the Catalytic Aspartic Acids

			ΔG_1° (kcal/mol)[c]					
					correction			
inhibitor (protonation states of the catalytic aspartic acids)[b]	k_{harm} (kcal/mol/Å^2)		ele	vdw	$-RT\ln\left(\frac{\sigma_{PLW}}{\sigma_{PL}\sigma_W}\right)$	$RT\ln\left[C^\circ\left(\frac{2\pi RT}{k_{harm}}\right)^{3/2}\right]$	total	$\Delta G^\circ = \Delta G_2^\circ - \Delta G_1^\circ$ (kcal/mol)[d]
KNI-272 (ASH25,ASP125)	10	F[a]	11.1	1.8	0.4	−5.3	8.0	
		B	10.4	2.0	0.4	−5.3	7.5	−1.9 ± 0.4
		avg					7.8 ± 0.3	
KNI-272 (ASP25,ASP125)	10	F	12.3	1.8	0.4	−5.3	9.2	
		B	12.1	1.7	0.4	−5.3	8.9	−3.2 ± 0.3
		avg					9.1 ± 0.2	
ABT-538 (ASH25,ASP125)	12	F	14.7	0.2	0.4	−5.4	9.9	
		B	14.5	0.6	0.4	−5.4	10.1	−4.1 ± 0.3
		avg					10.0 ± 0.2	
ABT-538 (ASP25,ASH125)	12	F	15.2	−0.4	0.4	−5.4	9.8	
		B	15.3	−0.8	0.4	−5.4	9.5	−3.8 ± 0.4
		avg					9.7 ± 0.3	

[a] F: forward; B: backward; avg: average. [b] ASH is the protonated aspartic acid. ASP is the unprotonated aspartic acid. [c] ele: the electrostatic component of the free energy change calculated by the electrostatic decoupling approach. vdw: the van der Waals interaction component of the free energy change calculated by the electrostatic decoupling approach. Correction: the calculated correction term corresponding to the ΔG_{corr} in eqs 4 and 5. [d] $\Delta G_2^\circ = 5.9 \pm 0.1$ kcal/mol, as in Table 1.

model compared with the crystal structure, and the near coplanarity of Asp25 and Asp125 observed in the crystal structure is lost. The distance between the proximal δ-oxygen atoms of Asp25 and Asp125 is 3.0 Å in the crystal structure and 3.1 Å in the averaged MD structure of (0, −1) model, whereas it is 3.8 Å in the averaged MD structure of (−1, −1) model. The negative charge of Asp25 in the (−1, −1) model creates repulsive forces acting on the P1 carbonyl oxygen of KNI-272, and as a result, the ligand P1 carbonyl oxygen moves toward the flap region (Figure 5), breaking the H bond formed with Asp25 in the crystal structure. The distance between the P1 carbonyl oxygen and the proximal δ-oxygen atom in Asp25 is 2.6 Å in the crystal structure, whereas it is 4.6 Å in the averaged MD structure of the doubly deprotonated model. As a consequence, the binding positions of the P1, P1′ moieties and the P2 carbonyl group of KNI-272, which have close contacts with Wat301, shift toward the flap region and deviate significantly from the crystal structure (Figure 5).

Accompanying the shift of the ligand, the flap tips of HIV-1 PR are also observed to be further removed from the base of the active site than in the crystal structure (Supporting Information). Therefore, the di-deprotonation states of the catalytic aspartic residues lead to considerable structure changes in the active site, the ligand, and the HIV-1 PR flap tips compared with the crystal structure and the monoprotonated model. Hence, di-deprotonation states of the Asp25/Asp125 lead to considerable changes in the binding environment of Wat301 and the overall active-site structure. Therefore, although there is no short-range interaction between Wat301 and these two aspartate residues in the protein, different protonation states of the Asp25/Asp125

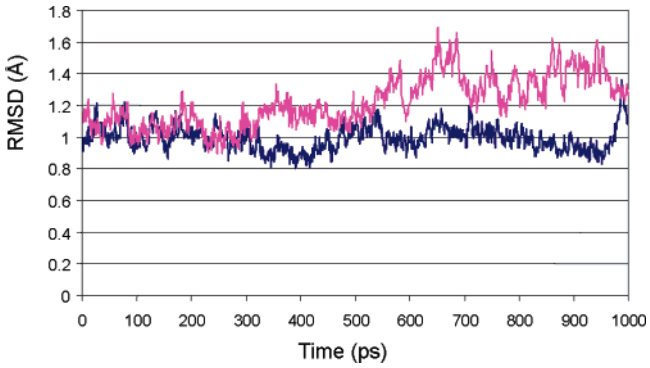

Figure 4. Root-mean-square deviation (RMSD) of the protein backbone atoms relative to the crystal structure of HIV-1 PR/KNI-272 complex during the 1-ns MD simulation, under two different protonation states of Asp25/Asp125. (Red): Dianionic model (−1, −1) in which both of the Asp25/Asp125 are deprotonated. (Blue): Monoanionic model (0, −1) in which Asp25 is protonated and Asp125 is anionic.

have a significant influence on the binding free energy contribution of Wat301.

It is of interest to note that the change of the protonation state of Asp25 also leads to different dynamic behaviors of two other crystal water molecules, Wat607 and Wat608. Wat608 is located at a peripheral cavity of the binding site in the crystal structure[13] and forms hydrogen bonds with the amide nitrogen atom of the KNI-272 P2′ group, the backbone nitrogen of Asp29, and the carbonyl oxygen of Gly27. However, in the MD simulation of the dianionic model (−1, −1), Wat608 is observed to migrate down from the peripheral area deep into the binding site, where it forms a hydrogen bond with the δ-O atom of the Asp25, thus shielding the negative charge of the Asp25 from the surrounding ligand and protein atoms (Figure 5). In the MD simulation of the (0, −1) model, Wat608 was observed to finally leave its original position and exchange with a solvent molecule. Another crystal water molecule, Wat607, is located at the S1 subsite of the protease in the crystal structure. Structurally Wat607 is stabilized by a hydrogen bond with the carboxyl group of the negatively charged catalytic acid Asp125 (Figure 2). During the MD simulation of the (0, −1) model, the position of Wat607 is very stable and close to its position in the crystal with a RMSD of 0.78 Å. However, in the dianionic model, Wat607 leaves its crystal position and moves to a position between Asp25 and Asp125, shielding the repulsion between the two COO^- groups (Figure 5). The RMSD of the Wat607 oxygen compared with the crystal structure is 4.32 Å. It is noted that the fourth crystal interfacial water molecule, Wat566, remains at its crystal position in both models, with a RMSD 1.34 Å in the (−1, −1) model and a RMSD 0.94 Å in the (0, −1) model.

Our MD simulations indicated that the crystal conformation of the HIV-1 PR/KNI-272 complex is very stable in the monoprotonation state for Asp25 and Asp125. When both Asp25 and Asp125 are deprotonated, the electrostatic repulsion between neighboring oxygen atoms causes considerable conformational change in the protein and ligand atoms and crystallographic water molecules compared with that in the crystal structure. The rearrangement of protease flap tips and the ligand in the dianionic state probably is the main cause of the difference in binding free energy of Wat301 under the different protonation states of Asp25 and Asp125.

Wat301 is found in almost all of the crystal structures of HIV-1 PR complexed with inhibitors. To investigate the influence of the bound inhibitor to the free energy contribution of Wat301, we have calculated the free energy contribution of Wat301 in the HIV-1 PR/ABT-538 complex. We have performed two independent simulations using two monoprotonation states for these two aspartate residues. In one simulation, Asp25 was treated as protonated (ASH), while Asp125 was treated as deprotonated (ASP). In the second simulation, Asp25 was treated as deprotonated (ASP), while Asp125 was treated as protonated (ASH). The results are summarized in Table 3.

As can be seen, the calculated ΔG_1° values are very similar under these two conditions, being 10.0 ± 0.2 kcal/mol under the ASH/ASP protonation condition for Asp25 and Asp125 residues and 9.7 ± 0.3 kcal/mol under the ASP/ASH protonation

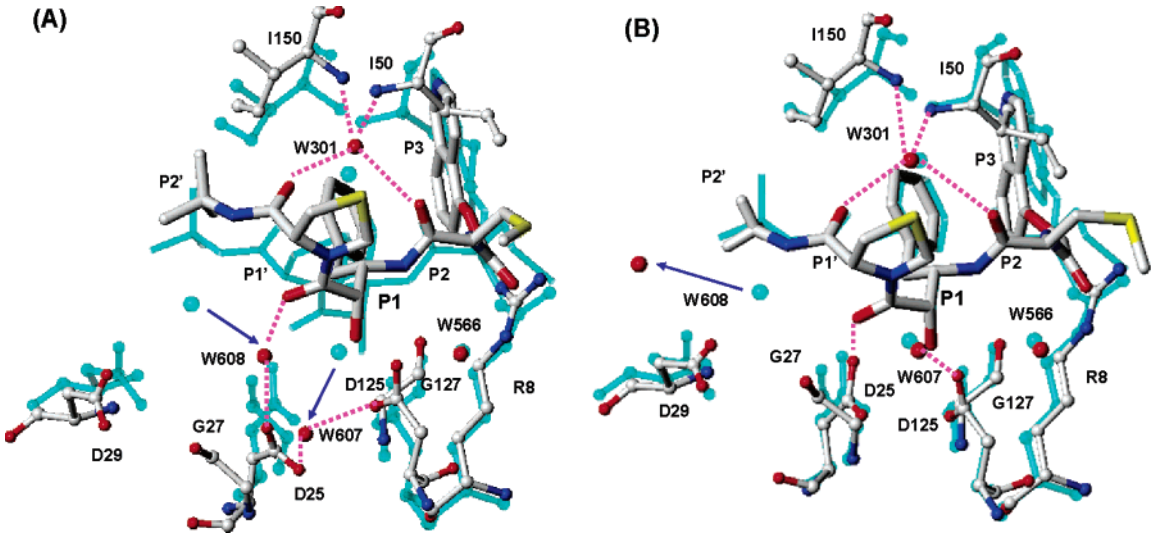

Figure 5. Superimposed active-site conformations of the averaged MD structure and the crystal structure of HIV-1 PR/KNI-272 complex (A) in the (−1, −1) model; (B) in the (0, −1) model. For the averaged MD structure, KNI-272 is shown as thick stick, and selected protein residues are shown as ball-and-stick, carbons in white, nitrogens in blue, oxygens in red, and sulfurs in yellow. The four interfacial crystal water molecules are shown as red balls. The selected hydrogen bonds formed between water and the complex are shown as purple dotted lines. For the crystal structure, KNI-272 is shown as a stick in cyan, and selected protein residues are shown as ball-and-stick in cyan. The four interfacial crystal water molecules are shown as balls in cyan. The position changes of Wat607 and Wat608 in the MD structure relative to the crystal structure are shown as blue arrows.

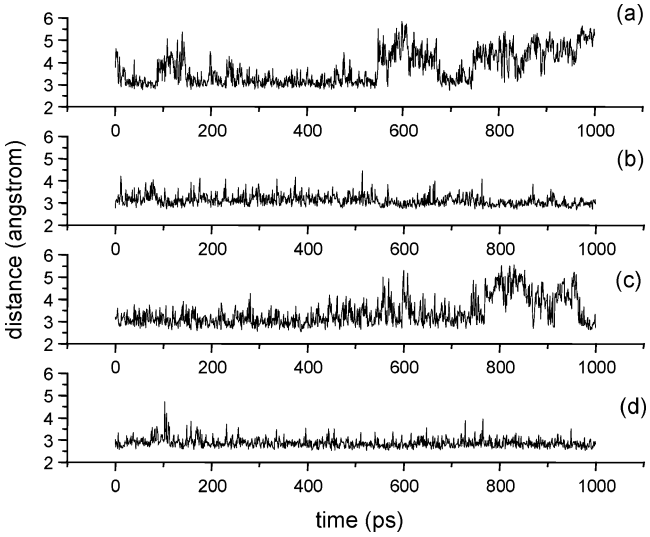

Figure 6. Hydrogen bond distance between the oxygen of the Wat30 1 and (a) the backbone nitrogen of Ile150; (b) the backbone nitrogen of Ile50; (c) the P2 carbonyl oxygen of KNI-272; (d) the P1′ carbonyl oxygen of KNI-272 in the 1-ns MD simulation of the HIV-1 PR/KNI-272 complex.

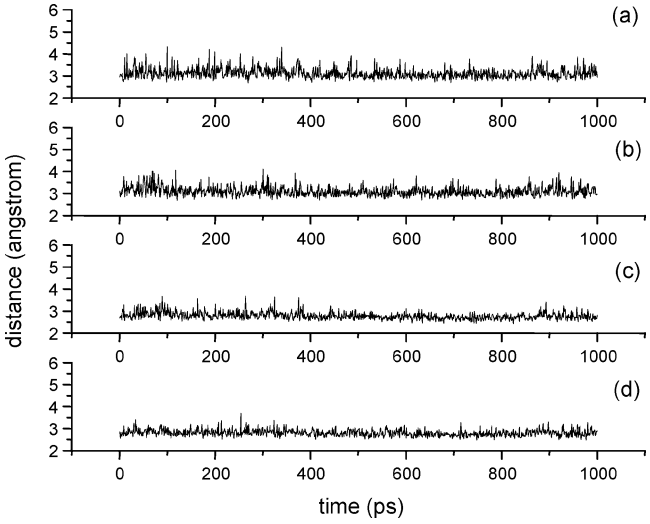

Figure 7. Hydrogen bond distance between the oxygen of the Wat301 and (a) the backbone nitrogen of Ile150; (b) the backbone nitrogen of Ile50; (c) the P1′ carbonyl oxygen of ABT-538; (d) the P2 carbonyl oxygen of ABT-538 in the 1-ns MD simulation of HIV-1 PR/ABT-538 complex.

condition for Asp25 and Asp125 residues, respectively. Hence, the free energy contribution for localizing Wat301 in the binding site of HIV-1 PR complexed with ABT-538 is -4.1 ± 0.3 kcal/mol when Asp25 is protonated and -3.8 ± 0.4 kcal/mol when Asp125 is protonated. Our calculations thus show that, on average, localization of Wat301 is 2.1 kcal/mol more favorable in the complex of HIV-1 PR/ABT-538 than in the complex of HIV-1 PR/KNI-272. These results suggest that the bound inhibitor in the HIV-1 PR complex has a significant influence on the free energy contribution by Wat301.

Wat301 forms four hydrogen bonds in both complexes, and the bound inhibitor can influence the free energy contribution from Wat301 by affecting these hydrogen bonds. We have therefore performed two 1-ns MD simulations on the HIV-1 PR/ABT-538 system with the monoprotontation states used in the free energy simulations and compared them to the 1-ns MD simulation performed on the HIV-1 PR/KNI-272 system. We have analyzed the four hydrogen bonds formed by Wat301.

Our analysis showed that both complex structures are stable and remain close to crystal structures during the 1-ns MD simulations. The RMSD of the protein backbone during the MD simulation relative to the crystal structure is 0.99 ± 0.08 Å for the HIV-1 PR/KNI-272 complex with Asp25/Asp125 monoprotonated at Asp25, and 0.99 ± 0.07 Å and 1.14 ± 0.08 Å for the HIV-1/ABT-538 complex under two different monoprotonation states. Figures 6 and 7 depict the donor−acceptor distances for the four hydrogen bonds formed by Wat301 in the HIV-1 PR/KNI-272 and HIV-1 PR/ABT-538 complexes, respectively.

As can be seen in Figure 6b, the hydrogen bond between the Wat301 oxygen and the NH of Ile50 was observed in 95% of the snapshots; the average donor−acceptor distance for this hydrogen bond is 3.1 ± 0.2 Å (3.0 Å in the crystal structure). In comparison, the hydrogen bond between the Wat301 oxygen and the NH of Ile150 was observed in only 57% of the snapshots (Figure 6a), and the average donor−acceptor distance for this hydrogen bond is 3.5 ± 0.2 Å, compared to 2.9 Å in the crystal structure, suggesting that this hydrogen bond is less stable than that between Wat301 and Ile50. As noted, there are more fluctuations in the distance between the Wat301 oxygen and the Ile150 backbone nitrogen after 550-ps simulation. A previous NMR study[14] of this complex indicated that Wat301−Ile50 has a larger cross-relaxation rate (i.e., $\sigma_{roe} = 7.54$) in the rotating frame than Wat301−Ile150 ($\sigma_{roe} = 6.97$). Since the value of σ_{roe} increases monotonically as the water residence time increases,[14] the NMR data suggests that there is a stronger interaction between Wat301 and Ile50 than that between Wat301 and Ile150, supporting the data obtained from our simulation. In our MD simulation of the HIV-1 PR/KNI-272 complex, the RMSD for the Ile50 backbone nitrogen is 0.57 Å, while the RMSD value for the Ile150 backbone nitrogen is 0.90 Å. This is also in agreement with a previous MD study that showed Ile150 to be more mobile than Ile50.[40] Thus, the hydrogen bond between Wat301 and Ile150 breaks more frequently and is less stable than that between Wat301 and Ile50, probably due to the increased positional fluctuation of Ile150. Wat301, functioning as a hydrogen bond donor, forms a hydrogen bond with the CO group of the KNI-272 P1′ site and another hydrogen bond with the CO group of the KNI-272 P2 site. On the basis of our simulation results, these two hydrogen bonds also appear to have different stabilities. The hydrogen bond between Wat301 and the CO group of the KNI-272 P1′ site was observed in 98% of the simulation trajectories (Figure 6d) and has an average donor−acceptor distance of 2.9 ± 0.2 Å (2.9 Å in the crystal structure). In comparison, the hydrogen bond between Wat301 and the CO group of the KNI-272 P2 site was observed in 71% of the simulation trajectories (Figure 6c) and has an average donor−acceptor distance of 3.4 ± 0.2 Å (3.0 Å in the crystal structure). Overall, the average number of hydrogen bonds observed between Wat301 and HIV-1 PR/KNI-272 during the 1-ns MD simulation is 3.2, primarily due to the reduced stability of the two hydrogen bonds formed by Wat301 with Ile150 and the carbonyl oxygen in the KNI-272 P2 site.

All four hydrogen bonds formed by Wat301 in the HIV-1 PR/ABT-538 complex were found to be very stable during our MD simulations (Figure 7). For example, in the simulation with

(40) Luo, X.; Kato, R.; Collins, J. R. *J. Am. Chem. Soc.* **1998**, *120*, 12410−12418.

the ASP/ASH monoprotonation state for Asp25/Asp125 residues, the two hydrogen bonds formed between Wat301 and Ile50 (Figure 7b) and Ile150 (Figure 7a) are both observed in 95% of the trajectories, with an average donor−acceptor distance of 3.1 ± 0.2 Å and 3.0 ± 0.2 Å (2.9 and 3.1 Å in the crystal structure), respectively. The other two hydrogen bonds formed between Wat301 and ABT-538 are also very stable and are found in essentially 100% of the snapshots, with an average donor−acceptor distance of 2.8 ± 0.1 Å and 2.8 ± 0.2 Å (2.7 and 2.6 Å in the crystal structure), respectively (Figures 7c and 7d). Similar results were obtained during the simulation with the ASH/ASP monoprotonation state for Asp25/Asp125 residues. Overall, the average number of hydrogen bonds observed between Wat301 and HIV-1 PR/ABT-538 is 3.9, compared to 3.2 for Wat301 in the HIV-1 PR/KNI-272 complex.

Therefore, the higher overall stability of the four hydrogen bonds formed by Wat301 in HIV-1 PR/ABT-538 complex suggests that there is a larger enthalpy gain when Wat301 is localized in the HIV-1 PR/ABT-538 complex than in the HIV-1 PR/KNI-272 complex. This may explain the greater free energy contribution from Wat301 in the HIV-1 PR/ABT-538 complex compared to that in the HIV-1 PR/KNI-272 complex.

Free Energy Contributions of Wat566, Wat607, and Wat608. Three other interfacial water molecules, namely Wat607, Wat566, and Wat608, are found in the binding site of the HIV-1 PR/KNI-272 complex in the crystal structure. Unlike Wat301, these water molecules are not identified as "conserved" because they are not found in all HIV-1 protease/ligand complexes.

The shallow binding of the thioproline moiety of KNI-272 in the S1′ subsite leaves room for a water molecule, Wat607, to occupy this subsite.[13] In the crystal structure of HIV-1 PR/ABT-538 complex, however, the P1′ moiety of ABT-538 projects more deeply into the S1′ subsite, and the water molecule corresponding to Wat607 is not observed. The calculated free energy of localization of Wat607 in HIV-1 PR/KNI-272 complex is −1.1 ± 0.3 kcal/mol (Table 2). This indicates that the localization of Wat607 is favorable. Structurally, Wat607 is stabilized by a hydrogen bond with the carboxyl group of the negatively charged catalytic acid Asp125. MD simulation indicates that this hydrogen bond is stable and observed in 99% of the snapshots with an average donor−acceptor distance of 2.7 ± 0.1 Å. Although no hydrogen bond is formed between Wat607 and KNI-272, this water molecule is in close contact with the thioproline ring in the inhibitor P1′ site,[13] with a distance of 3.3−3.9 Å from the oxygen atom of Wat607 to all the thioproline ring atoms.

Both Wat301 and Wat607 are completely buried inside the binding pocket and inaccessible to other water molecules. In contrast, Wat566, together with another water molecule (Wat406), is trapped in a narrow polar cavity between HIV-1 PR and KNI-272. Wat566 participates in a hydrogen-bonding network with Nδ of Arg8, the carbonyl oxygen of Gly127, the carbonyl oxygen in P3 of KNI-272 and also Wat406. The isoquinoline group of the KNI-272 P3 moiety is packed above Wat566, forming a lid for this narrow cavity. When HIV-1 PR binds with different inhibitors, the size of this cavity is adjusted to accommodate either one or two water molecules, depending upon the inhibitor.[41] The free energy of localization of Wat566 is calculated to be 0.4 ± 0.5 kcal/mol. Our data thus suggest that, although Wat566 participates in an extensive hydrogen bond network with HIV PR and KNI-272, localization of this water at this site does not contribute favorably to the binding free energy. Hence, from our data, it appears that the main role of Wat566 is primarily structural, supporting the formation of the hydrogen-bonding network. A water molecule, Wat52 in a similar position to that of Wat566 is observed in the crystal structure of HIV-1 PR/ABT-538 complex. While Wat566 in HIV-1 PR/KNI-272 complex has close contacts and forms hydrogen bonds with both protein and inhibitor, Wat52 in HIV-1 PR/ABT-538 only forms a hydrogen bond with the HIV-1 PR but not with the inhibitor. ABT-538 does not have a moiety corresponding to P3 in KNI-272, which is in close contact with Wat566 and traps the water molecule in the polar pocket. Our MD study indicated that, while Wat566 is stable and remains close to its crystal position through the 1-ns MD simulation of the HIV-1 PR/KNI-272 complex, Wat52 in the HIV-1 PR/ABT-538 complex is observed to escape to solvent and exchange position with a solvent water molecule. Therefore, although Wat566 and Wat52 have similar positions, their binding environments are quite different, and they are not equivalent in these two complex structures.

Wat608 is located at a peripheral area of the binding site and in the crystal structure.[13] It forms hydrogen bonds with the amide nitrogen atom of the KNI-272 P2′ group, the backbone nitrogen of Asp29, and the carbonyl oxygen of Gly27. In the crystal structures of HIV-1 PR with larger inhibitors, the position of Wat608 is occupied by the carbonyl oxygen of the P2′−P3′ amide.[15,17,42,43] For example, the position of Wat608 in HIV-1 PR/ABT-538 complex is occupied by the carbonyl oxygen of the P3′ amide in ABT-538,[17] and therefore a water molecule equivalent to Wat608 in the HIV-1 PR/KNI-272 complex is not observed in the crystal structure of HIV-1 PR/ABT-538 complex. Compared with the other three water molecules that are buried inside the complex, Wat608 makes contact with the first shell of the solvent at a peripheral area of the binding site. In our MD simulation, it was observed that after 200 ps, Wat608 leaves its original position and diffuses to the solvent. At the same time, another solvent water molecule enters and occupies the Wat608 site. In contrast to the other three interfacial water molecules, Wat608 is mobile and can exchange positions with solvent water molecules. Therefore, in this study, only the first 200-ps MD simulation—before Wat608 diffuses to the solvent—was used to calculate the positional fluctuation of the oxygen atom and the harmonic force constant of Wat608. Furthermore, after the forward simulation, the end configuration is used as the starting configuration of the backward simulation without further reequilibration, to prevent other water molecules from entering the Wat608 site. The calculated binding free energy for Wat608 is −0.3 ± 0.3 kcal/mol. These data suggests that localizing Wat608 at its crystallographic position is only marginally favorable to the total binding free energy.

A recent study of the structural water molecules in 23 HIV-1 PR-inhibitor complexes using the HINT (Hydropatic INTeractions) scoring function has been reported.[44] HINT is an empirical

(41) Hosur, M. V.; Bhat, T. N.; Kempf, D. J.; Baldwin, E. T.; Liu, B. S.; Gulnik, S.; Wideburg, N. E.; Norbeck, D. W.; Appelt, K.; Erickson, J. W. *J. Am. Chem. Soc.* **1994**, *116*, 847−855.
(42) Tyndall, J. D.; et al. *J. Med. Chem.* **2000**, *43*, 3495−504.
(43) Chen, Z.; Li, Y.; Chen, E.; Hall, D. L.; Darke, P. L.; Culberson, C.; Shafer, J. A.; Kuo, L. C. *J. Biol. Chem.* **1994**, *269*, 26344−26348.

method used to calculate the binding free energy for protein−ligand systems.[45] It was shown that the inclusion of water molecules corresponding to Wat566 and Wat608 (Water 313 and Water 313′ in their study) did not improve the correlation between the HINT scores and the experimentally determined binding constants, while inclusion of Wat301 improved the correlation significantly.[44] This is consistent with our observation that Wat301 contributes significantly to the HIV-1 PR/KNI-272 association, while the contributions of Wat566 and Wat608 are minimal.

Limitations with Our Free Energy Calculations. The Amber force field (version 1999) used in the present study is an effective two-body additive force field. It has been shown to treat hydrogen bonding with reasonable accuracy via the combination of the Coulombic and LJ terms.[49] The charges have been derived using the 6-31G* basis set which overestimates the dipolar moment for implicit polarization simulations with the TIP3P water model.[49,50] The major limitation is that there is no explicit treatment of polarization and the atomic charges are fixed. Therefore, such a model is unable to respond directly to the molecular environment. However, despite the absence of explicit polarization interactions, effective two-body potentials have been shown to be very successful to simulate biomolecular systems.[46,47] At the present time, there is an intense effort to develop a new generation of force fields that would explicitly include induced polarization.[48,51] However, the behavior of polarizable force fields for flexible molecules is not yet completely understood, and polarizable force fields are yet to be validated. Once such validation is done, it will be highly desirable to investigate the effect of polarization on the free energy contribution for individual interfacial water molecules.

In free energy calculation, given a reliable force field, the largest source of error would be insufficient sampling. For complex biomolecular systems, however, it is difficult to know if configuration sampling is adequate. Here for each free energy calculation we performed two runs, one in the forward direction and one in the backward direction. The calculated free energy change is reported as an average of the forward and backward runs, and the estimated error is taken to be half of the difference between forward and backward runs (hysteresis). This error estimation provides a lower bound estimate of the error in a given free energy difference. A more reliable way would be running the simulation in even longer simulation length and performing multiple runs with different but equivalent starting configurations. This method probably provides the best estimation of the error and insurance that convergence has been reached, but it is still not definitive, and it is also the most costly and may be too computationally expensive to afford.

(44) Fornabaio, M.; Spyrakis, F.; Mozzarelli, A.; Cozzini, P.; Abraham, D. J.; Kellogg, G. E. *J. Med. Chem.* **2004**, *47*, 4507−4516.
(45) Kellogg, G. E.; Burnett, J. C.; Abraham, D. J. *J. Comput.-Aided Mol. Des.* **2001**, *15*, 381−393.
(46) Pettitt, B. M.; Smith, J. C. *Comput. Phys. Commun.* **1995**, *91*, 1−344.
(47) van Gunsteren, W. F.; Berendsen, H. J. C. *Angew. Chem., Int. Ed. Engl.* **1990**, *29*, 992−1023.
(48) Ponder, J. W.; Case, D. A. *Adv. Protein Chem.* **2003**, *66*, 27−85.
(49) Cornell, W. D.; Cieplak, P.; Bayly, C. I.; Gould, I. R.; Merz, K. M., Jr.; Ferguson, D. M.; Spellmeyer, D. C.; Fox, T.; Caldwell, J. W.; Kollman, P. A. *J. Am. Chem. Soc.* **1995**, *117*, 5179−5197.
(50) Wang, J.; Cieplak, P.; Kollman, P. A. *J. Comput. Chem.* **2000**, *21*, 1049−1074.
(51) Mackerell, A. D., Jr. *J. Comput. Chem.* **2004**, *25*, 1584−1604.

Summary

Experimental determination of the free energy contribution from individual crystallographic interfacial water molecules to protein−ligand binding is difficult. Although high-resolution X-ray crystal structure and NMR spectroscopy have clearly shown the presence of these four interfacial water molecules in the HIV-1 PR/KNI-272 system, their precise contribution to the free energy of binding is not known. Our study has provided a theoretical prediction for the contribution for each of these four different interfacial water molecules observed in crystal and solution structures. Importantly, we have also analyzed the factors that influence the contribution for a conserved water molecule Wat301.

Employing the double-decoupling free energy and MD simulations, we have investigated the contribution of crystallographic interfacial water molecules to the total binding free energy using HIV-1 PR/KNI-272 and HIV-1 PR/ABT-538 as model systems. Our results show that the conserved Wat301 contributes significantly to the binding free energy in both systems. The calculated free energy contribution for Wat301 is strongly influenced by the protonation states of two catalytic Asp25 and Asp125 residues, likely due to the considerable structure changes in the binding environment of Wat301 caused by the di-deprotonation states of the aspartate dyad. Furthermore, the inhibitor bound to HIV-1 PR can have an important effect on the free energy contribution of Wat301, as exemplified by the 2.1 kcal/mol difference between the free energy contributions of HIV-1 PR/ABT-538 and the HIV-1 PR/KNI-272 complexes. This large difference in free energy contribution by Wat301 between these two complexes can be attributed to the different stabilization effect of the inhibitor on Wat301, as reflected by the strengths of four hydrogen bonds formed between Wat301 and the system shown in our MD simulations. Wat607 was found to make a significant and favorable contribution to the binding free energy, although smaller than that for Wat301. In contrast, the other two interfacial water molecules, Wat566 and Wat608, make minimal contribution to the binding free energy. Our study thus shows that contribution from individual crystallographically observed interfacial water molecules to the total free energy of protein−ligand binding varies considerably. Furthermore, the local environment such as protonation states of protein residues and bound inhibitor strongly influences the free energy contribution from an interfacial water molecule. Our study indicates that an in-depth understanding of the binding free energy contribution of individual crystallographic water molecules will have significant impact for accurate theoretical and computational binding affinity prediction and for structure-based drug design.

Acknowledgment. We are grateful to Dr. George W. A. Milne for his critical reading of the manuscript and his editorial assistance. We thank Dr. Donald Hamelberg for valuable discussion for the double decoupling free energy simulation method and the Center for Advanced Computing at the University of Michigan and Jianjun Yu for computing support.

Supporting Information Available: Complete citations for references 15, 16, 18, 23, 24, 26, 30, and 41. This material is available free of charge via the Internet at http://pubs.acs.org.

JA058042G